Modification of ZrN/Ti-6Al-4V system structure by compression plasma flows treatment

N.N. Cherenda [1]*, N.V Bibik[1], V.V. Uglov [1], S.N. Grigoriev [2], A.A. Vereschaka [3], V.M. Astashynski [4], A.M. Kuzmitski [4]

[1]Belarusian State University, Nezavisimosti ave. 4, 220030 Minsk, Belarus
[2]Moscow State University of Technology “STANKIN”, Vadkovsky Lane 3a, 127055 Moscow, Russia;
[3]Institute of Design and Technological Informatics of the Russian Academy of Sciences (IDTI RAS), Vadkovsky Lane 18a, 127055 Moscow, Russia;
[4]A.V.Lykov Heat and Mass Transfer Institute of the National Academy of sciences of Belarus, P. Brovka str. 15, 220072 Minsk, Belarus;
*****Correspondence: Tel.: +375172095590; Fax: +3752095445; E-mail: cherenda@bsu.by

Abstract:

Investigation of compression plasma flows impact on structure, phase and elemental composition as well as mechanical properties of Ti-6Al-4V titanium alloy with ZrN coating was carried out in this work. X-ray diffraction, scanning electron microscopy, energy dispersion X-ray analysis, samples weight measurements, microhardness and tribological tests were used as investigation techniques. The findings showed that plasma impact led to the formation of a composite surface layer based on titanium alloy containing inclusions of undissolved ZrN coating. Growth of the absorbed energy density resulted in a decrease of zirconium and nitrogen concentration in the the surface layer due to erosion. Formation of solid solutions on the basis of α-Ti and β-Ti was found in the layer analyzed by X-ray diffraction. Presence of nitrogen in a vacuum chamber as plasma generating gas led to the formation of TiN on the surface. Plasma impact resulted in decrease of ZrN/Ti-6Al-4V system microhardness and decrease of friction coefficient (at specific treatment regimes).

Keywords: titanium alloy; hard coating; compression plasma flows; phase composition; microstructure; erosion; microhardness; friction coefficient

1. Introduction

Titanium alloys possess high specific strength, good corrosion-resistance and biological response, relatively high static and fatigue strength (Brunello et al., 2018; Chen and Thouas, 2015; Fattah-alhosseini et al., 2023; Koshuro et al., 2023; Petrov et al., 2018). However, the applications of titanium alloys have been limited due to their low hardness and poor wear resistance (Fattah-alhosseini et al., 2023; Koshuro et al., 2023; Petrov et al., 2018). These limitations can be overcomed by application of an appropriate surface engineering method, in particular, hard coating deposition (Fattah-alhosseini et al., 2023; Koshuro et al., 2023; Petrov et al., 2018).

At the same time usage of hard coatings also have some drawbacks. PVD techniques widely used for hard coating deposition may result in formation of droplets and pores on the coatings surface and excessive residual stress in the as-deposited coating (Guan et al, 2024). The latter effect can lead to coating delamination (Guan et al, 2024). Coating produced by plasma spraying showed heterogeneity of the structure, high porosity and low adhesive strength (Koshuro et al., 2023). Besides that hard coatings often could not demonstrate high exploitation properties being deposited on relatively soft materials as titanium alloys so that an additional treatment of the substrate materials before or after coating deposition is necessary (Zenker et al., 2007; Weigel et al., 2014).

Thermal treatment of coating/substrate system is the easiest treatment type. In (Koshuro et al., 2023) it was shown that induction heat treatment of titanium with titanium oxide coating deposited by atmospheric plasma spraying resulted in increase of the coating microhardness and adhesive strength improvement . The usage of electron (Guan et al., 2024; Weigel et al., 2014; Schulz et al., 1991; Zenker et al., 2007; Arroyo et al., 2010; Petrov et al., 2018; Proskurovsky et al., 2000), ion (Manory et al., 1994), laser (Fattah-alhosseini et al., 2023; Zhang et al., 2020; Chengwen et al., 2024; Szajna et al., 2024; Arroyo et al., 2010) and plasma (Niksefat and Mahboubi, 2024; Mirhosseini et al., 2024; Sharma et al., 2023; Grigoriev et al., 2024; Cherenda, Leivi et al., 2024; Cherenda, Petukh et al., 2024) beams opens up wider possibilities for modifying the properties of the coating/substrate system.

Heating of the surface layer during electron beam treatment is one of the main effects providing modification of the surface layer properties. Using an electron beam, a localized heat treatment of the sample can be applied and the heating rate as well as final temperature can be chosen over a wide range (Schulz et al., 1991; Zenker et al., 2007). That is why the substrate material is not heated up to critical temperatures worsening base material properties (Zenker et al., 2007). Thermal effect provides diffusion enhancement in the interface region between the coating and substrate leading to an improved adhesion of TiAlN coating after treatment (Guan et al., 2024;

Weigel et al., 2014). Increase of the energy deposited in the surface layer during high current pulsed electron beam impact also led to TiAlN coating grain refinement due to surface layer melting and adjustment of residual stresses that were responsible for the improvement in both mechanical and tribological properties of the TiAlN coatings (Guan et al., 2023). Electron beam treatment due to high heating and cooling rates can facilitate formation of non-equilibrium microstructures exhibiting increased hardness (Buchwalder and Zenker, 2019). Besides thermal effects, the growth and stoichiometry of the coatings can be influenced by alternating sequences of heating and deposition (Schulz et al., 1991). Electron beam treatment of substrate material before coating deposition also can be effective for coating/substrate system properties modification. In (Petrov et al., 2018) it was shown that treatment of Ti5Al4V substrates before TiN/TiO_2 coatings deposition led to the transformation of α+β to α′ martensitic microstructure and the decrease of the coating friction coefficient.

Laser treatment of coating/substrate system is especially effective in melting mode (Chengwen et al., 2024; Fattah-alhosseini et al., 2023; Koshuro et al., 2023; Szajna et al., 2024). The laser melting resulted in enhancement of metallurgical quality of the coating and increase of it hardness and tribological properties (Chengwen et al., 2024; Szajna et al., 2024). In (Szajna et al., 2024) it was mentioned that amount of energy deposited in the surface layer is a crucial factor influencing on the microstructure and, hence, surface properties. Laser treatment of substrate material before coating deposition can also be applied (Arroyo et al., 2010; Zhang et al., 2020). In this case change of surface morphology and structure of substrate material is observed resulting in coating adhesion and wear resistance increase (Arroyo et al., 2010; Zhang et al., 2020).

Low-temperature plasma is mainly used for saturation of coatings by atoms of gas used for plasma generation, e.g. plasma nitriding (Niksefat and Mahboubi, 2024; Abdi et al., 2023; Mirhosseini et al., 2024; Sharma et al., 2023). Changes of coatings elemental and phase composition, as well as microstructure led to improvement of tribological properties (Mirhosseini et al., 2024; Niksefat and Mahboubi, 2024;), corrosion resistance (Abdi et al., 2023), hardness (Mirhosseini et al., 2024) and coating adhesion (Sharma et al., 2023). Low-temperature plasma pretreatment of substrate before coating deposition can also be used for adhesion enhancement (Grigoriev et al., 2024). It should be noted that preliminary treatment of substrate material by ion, electron and plasma beams that lead to surface roughness growth can result in increase of coating adhesion properties (Proskurovsky et al., 2020; Remnev et al., 1999; Leyvi and Yalovets, 2017).

Influence of high temperatre plasma flows impact on surface relief of Ti-6Al-4V titanium alloy and adhesion of ZrN coating to modified surface layer was considered in (Cherenda, Leivi et al., 2024; Cherenda, Petukh et al., 2024). The findings showed that plasma impact led to the formation of developed surface relief due to the action of hydrodynamic instabilities at the melt-plasma border. Formation of titanium nitride on the surface was observed as a result of the interaction of nitrogen (as a plasma generating gas) with the surface heated under plasma impact (Cherenda, Leivi et al., 2024). These effects influenced on coating – substrate interface areas. Scratch test of ZrN/Ti-6Al-4V system showed that preliminary plasma processing provided a higher critical force indicating adhesion properties improvement (Cherenda, Petukh et al., 2024).

Literature review showed that treatment of coating/substrate system by electron and laser beams in the melting mode led to substantial modification of system properties. It is known that compression plasma flows (CPF) treatment of the target material led also to it melting; initiation of hydrodynamic instabilities and appearance of convection mass and heat transfer flows in the melt; crystallization in conditions of superfast cooling of the melt (up to 10^7 K/s) after the end of plasma pulse (Cherenda, Leivi et al., 2024). From this point of view treatment of coating/substrate system by CPF could be promising modification technique. Thus investigation of the elemental and phase composition, structure and mechanical properties of the ZrN/Ti-6Al-4V system after CPF impact was the main aim of this work.

2. Experimental

The samples of Ti-6Al-4V titanium alloy (Grade 5) were used for investigations. This alloy is one of the most widely used titanium alloy for orthopedic and dental applications (Brunello et al., 2018) and satisfies the main requirements for metallic implants: biocompatibility, corrosion resistance, suitable mechanical properties and good osseo-integration (Chen and Thouas, 2015). The diameter of the samples was 25 mm, their thickness – 3 mm.

ZrN coating was deposited by vacuum arc deposition technique with controlled movement of cathode spot from Zr cathode in nitrogen atmosphere (Grigoriev et al., 2023; Vereschaka et al., 2020). Cleaning of the surface by Zr ions was carried out before deposition resulting in formation of thin (~ 50 nm) metal sublayer. ZrN coating thickness was about 3 μm.

Compression plasma flows treatment of ZrN/Ti-6Al-4V samples surface was carried using a gas-discharge quasi-stationary plasma accelerator: magneto-plasma compressor of compact geometry powered with the capacitive storage of 1200 mF, operating at the voltage of 4 kV. Nitrogen was used as a plasma-forming gas. The pressure in the pre-evacuated vacuum chamber was 10^{-3} Pa. The pressure of plasma-forming gas was 400 Pa. The discharge duration amounts to 100 μs. The density of energy absorbed by the surface layer (Q) of the target was changed in the range of 30-

43 J/cm^2 per pulse (registered by calorimetric measurements). Treatment was carried out by 3 pulses at the interval of 3-5 s.

The surface morphology of the samples was studied using scanning electron microscopy (SEM) on a LEO1455VP microscope combined with an Oxford X-ray detector for energy-dispersion X-ray microanalysis (EDX). The phase composition of the surface layer was investigated by means of the X-ray diffraction method (XRD) using the Ultima IV RIGAKU diffractometer in Bragg-Brentano geometry with parallel beams in Cu Kα radiation. The samples weight was determined before and after CPF treatment by analytical balance RADWAG AS 60/220/C/2/N with the accuracy of ±0.05 mg. Microhardness measurements were performed using a Vickers 402MVD Instron Wolpert Wilson Instruments semiautomatic microhardness tester at a load of 0.1 N. The time of measurement under load was 10 seconds. Tribological tests were performed using a UIPT-001 tribometer under dry friction conditions with reciprocating motion of an indenter made of WC alloy (8 wt.% of Co). The indenter speed was 2 mm/s, load on the indenter was 0.5 N. The tests were performed at room temperature with a relative air humidity of 40-50%.

3. Results and Discussion

Coating/substrate system is heterogeneous system. The impact of CPF on such systems, where coating and substrate materials are metals, should lead to the formation of a surface modified layer with a relatively uniform distribution of coating and substrate components (Cherenda et al., 2019). This is due to the fact that the high energy transferred by the plasma flow to the surface ensures the melting of the coating and the surface layer of the substrate. Hydrodynamic instabilities that arise at the plasma-melt boundary create conditions for convective mass transfer leading to homogenization of the elemental composition in such systems (Leyvi et al., 2017). Therefore, the closer the thermophysical characteristics of the coating and substrate materials are, the more uniform the distribution of elements in the modified layer will be. For the case considered in this work, when the melting temperatures of the ZrN coating (2980 ^{o}C) and the Ti-6Al-4V substrate material (1660 ^{o}C) are significantly different, the modified layer will be characterized by a non-uniform distribution of elements.

Figure 1 shows the surface morphology of ZrN/Ti-6Al-4V system samples before and after CPF treatment. On the surface of the coating before plasma impact droplet phase was observed, characteristic of the coating application method used (Figure 1a). CPF treatment with Q=30 J/cm^2 did not lead to melting of the entire volume of the coating (Figure 1b). Melting of the substrate titanium alloy and resulting cracking of the ZrN coating were observed. Areas of coating are clearly visible in photographs due to the elemental contrast used in SEM studies (backscattered electrons). Areas containing coating or zirconium atoms appear lighter due to the higher mass of zirconium atoms compared to titanium atoms. This was confirmed by EDX analysis. Figure 2 shows the distribution of elements along a line, which makes it possible to clearly identify areas of surface morphology with different elemental contrast. It should be noted that on the surface of the rupture area between the parts of ZrN coating (Figure 2a), the presence of nitrogen with a concentration of up to ~ 20 at.% was observed (Figure 2b). Presence of Zr atoms was also observed in this region indicating that some mixing of coating and substrate material occured.

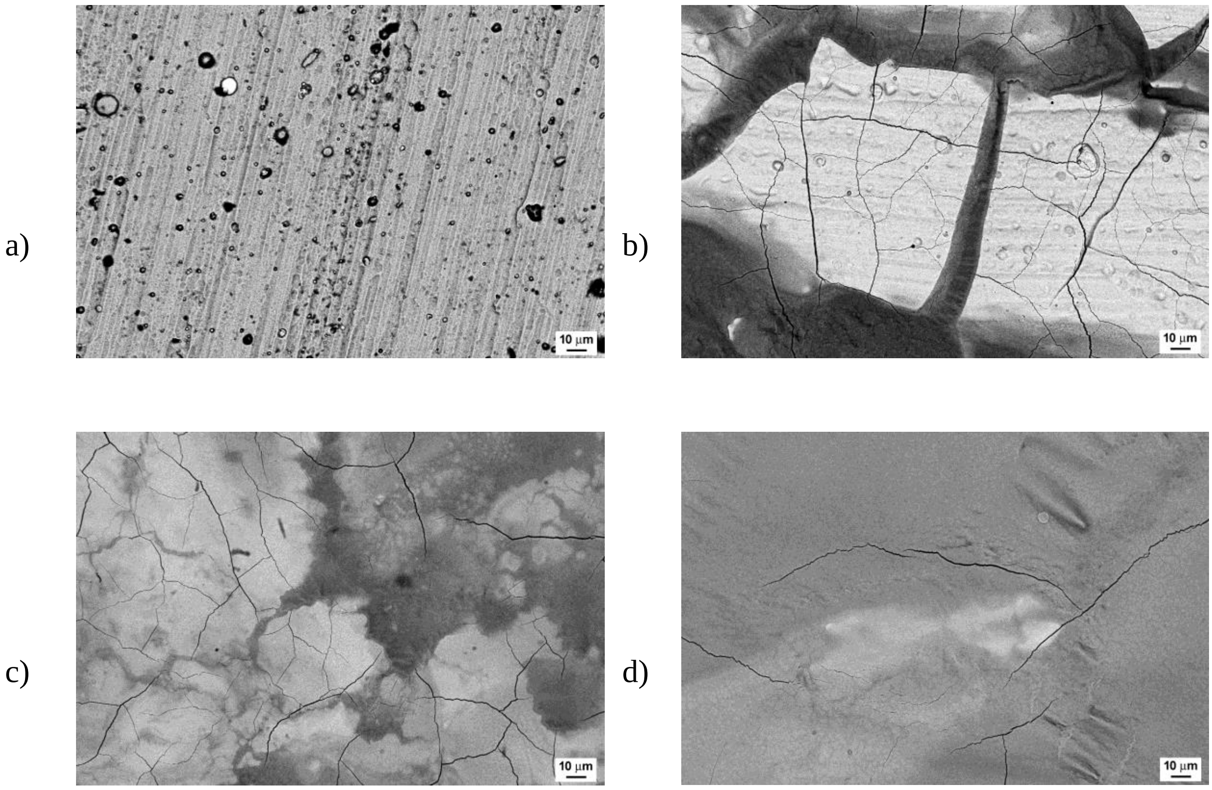

Figure 1. Surface morphology of ZrN/Ti-6Al-4V samples before (a) and after CPF treatment with Q=30 J/cm^2 (b), Q=37 J/cm^2 (c), Q=43 J/cm^2 (d).

a) b)

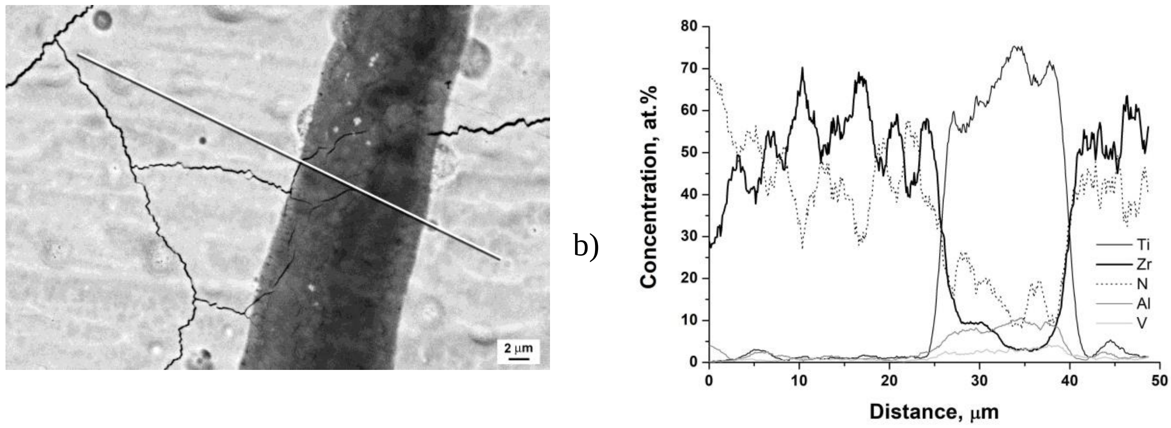

Figure 2. Surface morphology (a) and elements distribution along line (b) in ZrN/Ti-6Al-4V sample after CPF treatment with Q=30 J/cm^2.

Growth of the absorbed energy density up to 37 J/cm^2 led to an increase in the degree of dissolution of the coating material in the substrate (Figure 1c). Elemental contrast becomes more uniform. Only separate areas enriched with zirconium atoms are observed on the surface with a further Q increase (Figure 1d). Cracks are still present on the surface under this treatment mode. In this case, their appearance was due to the formation of regions of different elemental composition in the melt with various densities and crystallization temperatures. During solidification, this effect led to a violation of the crystallized material volume continuity.

The results of elemental analysis carried out from the surface of the sample using EDX are presented in Figure 3. The figure shows the dependence of the average concentration of elements over the surface area (at magnification x200) in a layer with a thickness of ~ 1 μm. In the initial sample with coating the concentrations of zirconium and nitrogen atoms were 61 and 39 at.%, respectively. CPF impact and an increase in absorbed energy density led to a decrease in the concentration of zirconium and nitrogen atoms in the analyzed layer. The concentration of nitrogen under all modes of treatment remained greater than the concentration of zirconium atoms. This may indicate additional saturation of the surface layer with nitrogen atoms from the residual atmosphere of the vacuum chamber (Cherenda et al., 2012). An increase in the absorbed energy density also resulted in an increase in the concentration of titanium alloy elements (Ti, Al, V) in the layer analyzed by EDX that is in accordance with SEM data (Figure 1).

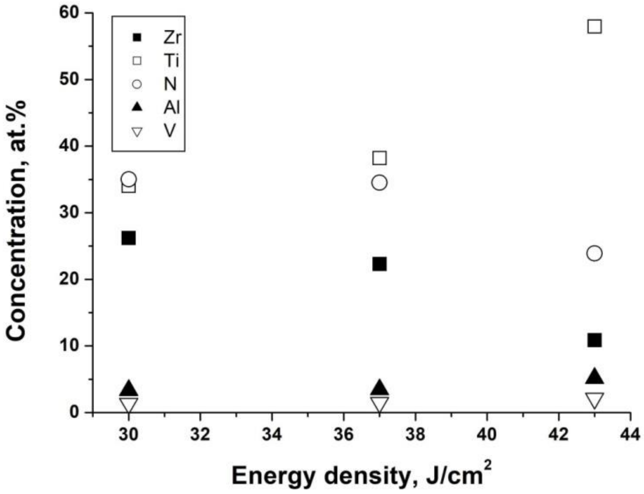

Figure 3. Dependence of elements concentration at the surface of the ZrN/Ti-6Al-4V samples treated by CPF on the energy density absorbed by the surface layer (EDX).

The main reasons of the coatings elements concentrations decrease in the surface layer after the CPF impact with Q growth are following (Cherenda et.al., 2015; Leyvi et.al., 2017; Cherenda et.al., 2019). The first reason is the increase in the melted depth and redistribution of all elements over the whole melted layer. Second one is the erosion of the surface. The existence of the surface erosion was confirmed by the measured mass loss of the samples after the CPF treatment (Figure 4). It can be seen from the figure that an increase in the absorbed energy density led to the growth of the erosion intensity. Comparison with removed mass data from Ti-6Al-4V alloy samples shows that the ZrN coating provides higher erosion resistance to high-temperature plasma impact.

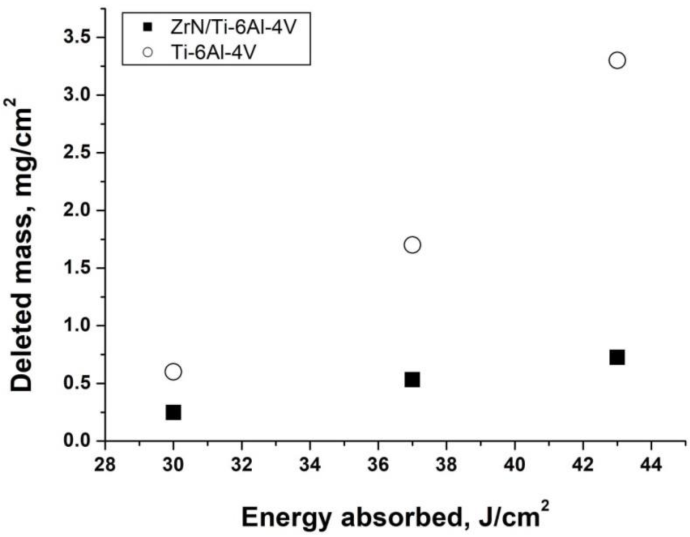

Figure 4. Dependence of the mass deleted from the square unit of Ti-6Al-4V and ZrN/Ti-6Al-4V samples on the energy density absorbed by the surface layer.

The hydrodynamic motion of the surface melt was the main reason of the erosion (Tereshin et.al., 2003; Cherenda et.al., 2015; Martynenko, 2015; Leyvi et.al., 2017). The plasma stream interacts with the target and spreads over the surface in radial directions that provides the melt ejection out of the sample. Increase of the energy density absorbed by the surface layer lead to the growth of melt existence time resulting in the rise of life time of this mechanism action. Presence of solid areas of ZrN coating in Ti-6Al-4V melt lead to decrease of the sample melted layer viscosity during impact. That is why erosion intensity of the coated with ZrN sample of Ti-6Al-4V alloy will be higher than that of uncoated sample.

The data of the phase composition analysis correlate with the data of SEM and EDX. According to the XRD results, the analyzed layer of the original coated sample contains diffraction lines of α-Ti with an hcp crystal lattice and ZrN with an fcc crystal lattice (Figure 5). The lattice parameter of ZrN is 0.4592±0.006 nm (Figure 6), which is greater than that of the standard - 0.4577 (JCPDS card #35-0753). A higher value of lattice parameter can be associated with the non-stoichiometry of the coating and the presence of macrostress. The CPF impact and an increase in the density of absorbed energy led to a decrease of ZrN diffraction lines intensity indicating diminishing of this phase content in the analyzed layer. After treatment with Q = 43 J/cm^2 diffraction lines of ZrN with very low intensity are observed. Thus CPF impact on the ZrN/Ti-6Al-4V system resulted in the formation of a composite surface layer based on titanium alloy containing inclusions of undissolved ZrN coating. XRD analysis also showed that CPF treatment led to a decrease of ZrN lattice parameter (Figure 6). After CPF treatment with Q = 30 J/cm^2, the lattice parameter corresponded to the standard value of the, which may indicate the removal of macrostresses during heating of the coating during plasma impact. However, with an increase in the absorbed energy density, the lattice parameter was decreased to a value of 0.4566±0.006 nm. Diffusion of titanium atoms from the melt into undissolved areas of the ZrN coating and the formation of a solid solution (Zr,Ti)N may be a possible reason of this effect. Since the atomic radius of titanium (0.146 nm) is less than the atomic radius of zirconium (1.620 nm), this should lead to a decrease in the crystal lattice parameter.

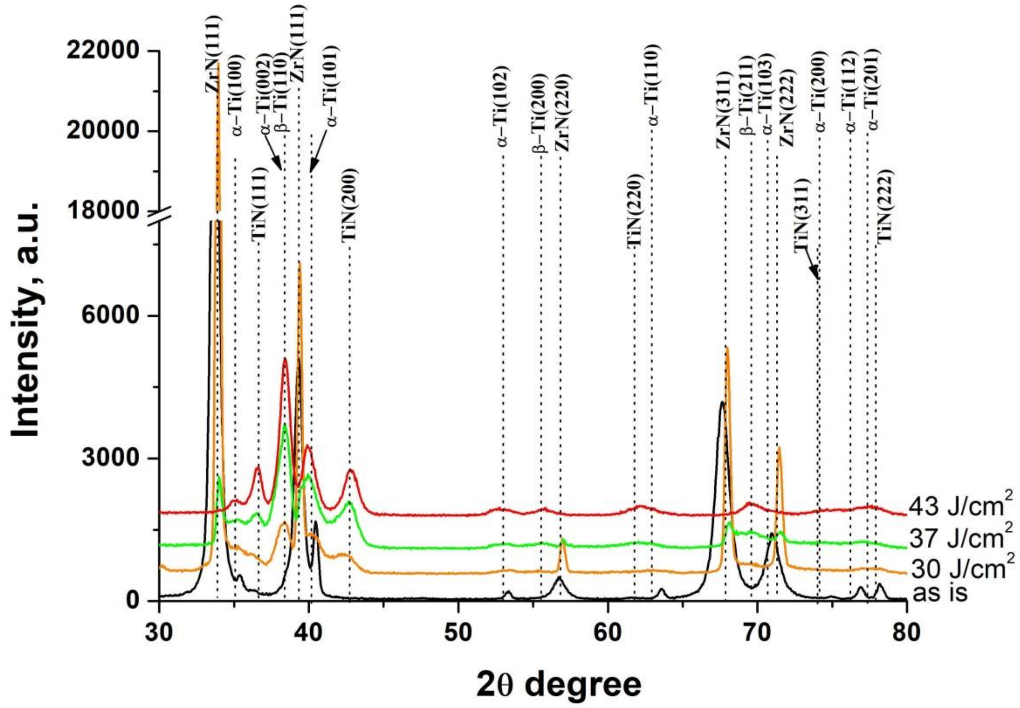

Figure 5. X-ray diffraction patterns of ZrN/Ti-6Al-4V samples before and after CPF treatment with different energy density absorbed by the surface layer.

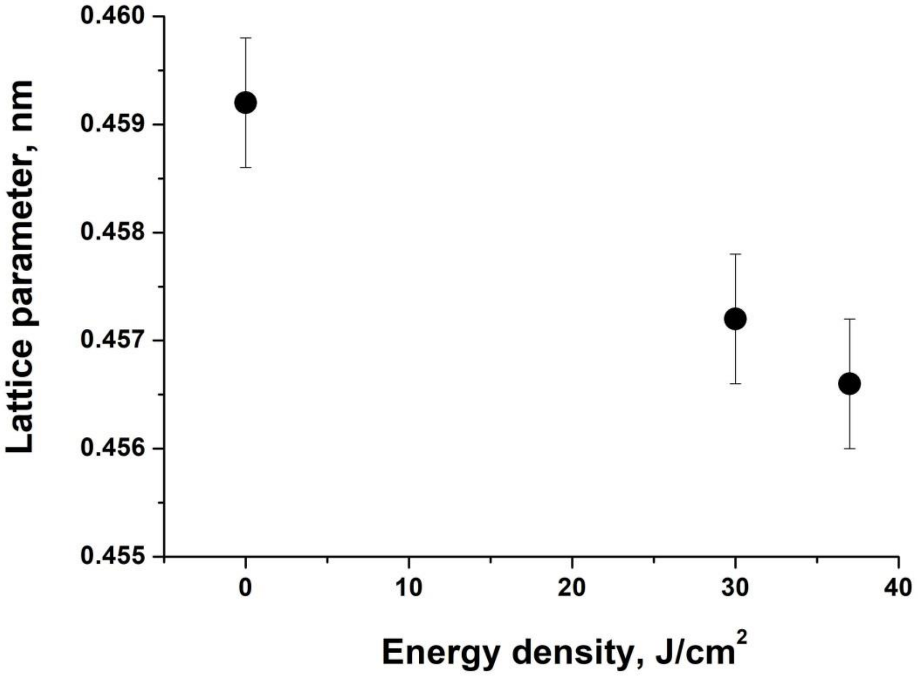

Figure 6. Dependence of ZrN lattice parameter of ZrN/Ti-6Al-4V samples on the energy density absorbed by the surface layer.

The diffraction patterns of the samples show the appearance of diffraction lines of TiN nitride with an fcc crystal lattice after CPF treatment (Figure 5). The reasons for the formation of titanium nitride under CPF exposure were discussed earlier (Cherenda et al., 2012; Cherenda, Leivi et al., 2024). During CPF generation, nitrogen is injected into the vacuum chamber thus leading to the formation of titanium nitride on the surface as a result of the interaction of gas atoms with the surface heated under plasma impact. The formation of titanium nitride should be observed in the surface areas free from the ZrN coating. As a result, the nitrogen concentration in the analyzed EDX layer will be higher than the nitrogen concentration in the original ZrN coating (Figure 3). The lattice parameter of the titanium nitride TiN formed after CPF impact is 0.4224 ± 0.0009 nm, which is less than the standard value of 0.4241 nm (JCPDS card #38-1420). This behavior may be associated with the formation of solid solutions based on TiN. In the initial state the basis of the Ti-6Al-4V alloy is a substitution solid solution α-Ti(Al,V). Since the radii of aluminum and vanadium atoms are smaller than the radius of titanium atoms, the solid solution of titanium with these elements has smaller crystal lattice parameters. After exposure, the nitride is formed on the basis of this solid solution, i.e. may contain both aluminum and vanadium atoms. A similar effect was observed in (Cherenda, Leivi et al., 2024). Besides that some of the zirconium atoms that appeared in the melt during dissolution of the ZrN coating could enter the ZrN melted areas during crystallization. Therefore, it would be more correct to assume the formation of a substitution solid solution Ti(Zr,Al,V)N with an fcc crystal lattice.

In (Cherenda, Leivi et al., 2024) it was shown that a decrease in the absorbed energy density leads to the growth of the intensity TiN diffraction peaks. The main reasons for such behavior were considered earlier (Cherenda et al., 2012). However, in this series of experiments, another regularity is observed – an increase of absorbed energy density led to an increase of the TiN diffraction lines intensity, which indicated an increase in its content in the surface layer. This is explained by an increase in the surface area of the titanium alloy subjected to nitriding with Q increase (Figure 1). This effect prevails over the effect described in (Cherenda, Leivi et al., 2024).

Zirconium atoms appearing in the melt during dissolution of the ZrN coating stimulatet the formation of other phases. The diffraction lines of α-Ti show the formation of “shoulders” after CPF treatment with Q=30 J/cm^2 (Figure 7). These “shoulders” can belong to the $Ti_{1.83}Zr_{0.17}$ phase (ICDD card # 1541222). It is a solid solution of zirconium (with a concentration of 8.5 at.%) in titanium with an hcp crystal lattice. The presence of an α-Ti(Zr) solid solution is also observed under other CPF treatment regimes (Figure 5). Besides that plasma impact also led to the formation of a solid solution based on β-Ti with a bcc crystal lattice (Figure 5). The intensity of this phase diffraction lines increases with a growth of the absorbed energy density. It is known that β-Ti phase can be observed at room temperature if it contains atoms of a stabilizing impurity with a concentration above the critical one. It can be assumed that under the conditions of this experiment β-Ti phase was stabilized by zirconium atoms. Under CPF impact ZrN coating was partially dissolved in the melt. Since the distribution of zirconium atoms is non-uniform (Figure 1), regions with different contents of zirconium atoms were formed in the melt. During crystallization of regions with a concentration below the critical one, a solid solution based on α-Ti was formed, and in regions with a concentration above the critical one, β-Ti was formed.

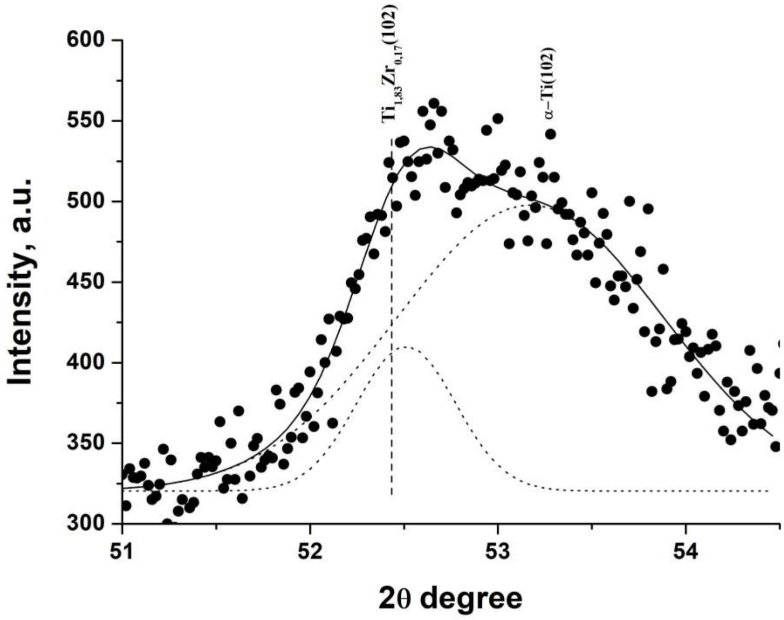

Figure 7. Part of X-ray diffraction pattern of ZrN/Ti-6Al-4V sample after CPF treatment with Q=30 J/cm^2.

Changes of ZrN/Ti-6Al-4V system structure and phase composition under CPF impact lad to a change in the mechanical and tribological characteristics of its surface layer. From Figure 8 it is evident that plasma action caused a decrease in microhardness from 9.5 GPa to 5-6 GPa, which is associated with the dissolution of the ZrN hard coating.

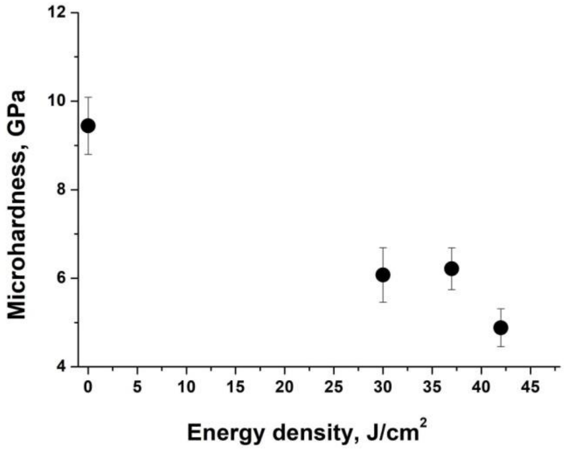

Figure 8. Dependence of ZrN/Ti-6Al-4V samples microhardness on the energy density absorbed by the surface layer.

The dependence of the friction coefficient on the Q is not monotonic (Figure 9). After treatment with Q = 30 J/cm^2, the friction coefficient increased from 0.153 to 0.167. However, a subsequent increase in Q led to a decrease in the friction coefficient to the value 0.13. This behavior may be associated with the formation of a structurally inhomogeneous surface containing inclusions of a hard coating in a soft matrix after treatment with Q = 30 J/cm^2. Such inclusions can act as an abrasive during friction increasing the contact area and friction force respectively. The formation of a more uniform surface, despite the decrease in microhardness, has a positive effect on the friction coefficient.

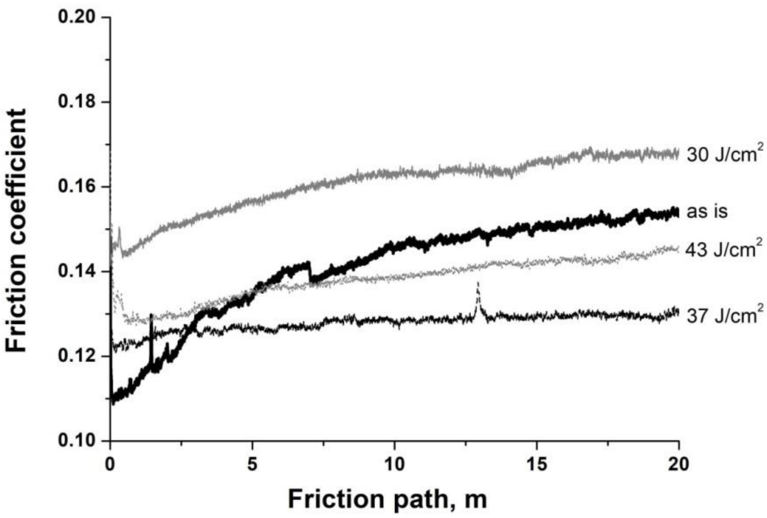

Figure 9. Dependence of ZrN/Ti-6Al-4V samples friction coefficient on the friction path before and after CPF treatment with different energy density absorbed by the surface layer.

All treatment regimes are characterized by a higher value of the initial friction coefficient compared to the untreated sample. This may be due to the formation of a developed surface relief after the action of CPF (Cherenda, Leivi et al., 2024), which increases the friction force during contact between the sample and the indenter.

4. Conclusions

Compression plasma flows impact (with the energy density absorbed by the surface layer 30-43 J/cm^2) on the ZrN/Ti-6Al-4V system led to the melting (partial melting) of the coating and the surface layer of the substrate and the formation of a composite surface layer based on titanium alloy containing inclusions of undissolved ZrN coating. Growth of the absorbed energy density resulted in a decrease of zirconium and nitrogen atoms concentration in the surface layer with the thickness of ~ 1 μm and more uniform distribution of elements. Surface erosion during plasma impact was one of the reasons influencing elements concentration behavior. An increase in the absorbed energy density led to the growth of the erosion intensity. Comparison with removed mass data from Ti-6Al-4V alloy samples showed that the ZrN coating provided higher erosion resistance to high-temperature plasma impact.

Zirconium atoms appearing in the melt during dissolution of the ZrN coating stimulated the formation of other phases. During crystallization of regions with Zr concentration below the critical one, a solid solution based on α-Ti was formed, and in regions with a concentration above the critical one, β-Ti was formed. The content of β-Ti phase increased with a growth of the absorbed energy density.

Presence of nitrogen in a vacuum chamber as plasma generating gas led to the formation of TiN on the surface of samples after plasma impact as a result of the interaction of gas atoms with the heated surface. TiN formation should be observed in the surface areas free from the ZrN coating. An increase of absorbed energy density resulted in an increase of TiN content at the surface layer. This is explained by an increase in the surface area of the titanium alloy subjected to nitriding with Q increase.

Changes of ZrN/Ti-6Al-4V system structure and phase composition under CPF impact led to a change in the mechanical and tribological characteristics of its surface layer. Plasma impact caused a decrease in a surface layer microhardness from 9.5 GPa to 5-6 GPa, which was associated with the dissolution of the ZrN hard coating. The dependence of the friction coefficient on the Q was not monotonic. Minimal value of friction coefficient 0.13 was found after treatment with Q=37 J/cm^2.

Acknowledgements

This work (experimental investigations) was supported financially by the Belarusian Republican Foundation for Fundamental Research (project no. T23RNF-228) and the Russian Science Foundation (project no. 23-49-10038).

References

Abdi, F., Aghajani, H., Tabrizi, A., Nasimi, L., Shokouhi, F., Study on the effect of the crack closing of AlCoCrFeMnNi high entropy alloy electro-spark deposited coating by plasma nitriding on the corrosion resistance, *Journal of Alloys and Compounds*, vol. **966**, p. 171629, 2023.

Arroyo, J. M., Diniz, A.E., Lima, M.S.F., Cemented carbide surface modifications using laser treatment and its effects on hard coating adhesion, *Surface & Coatings Technology*, vol. **204**, pp. 2410–2416, 2010.

Brunello, G., Brun, P., Gardin, C., Ferroni, L., Bressan, E., Meneghello, R., Biocompatibility and antibacterial properties of zirconium nitride coating on titanium abutments: An in vitro study. *PLoS ONE*, vol. **13**, no 6, p. e0199591, 2018.

Buchwalder, A., Zenker, R., Pre- and post-surface treatments using electron beam technology for load-related application of thermochemical and PVD hard coatings on soft substrate materials, *Surface and Coatings Technology*, vol. **375**, pp. 920-932, 2019.

Chen, Q., Thouas, G. A., Metallic implant biomaterials. *Mater. Sci. Eng. R*, vol. **87**, pp. 1–57, 2015.

Chengwen, S., Dejun, K., Effects of *in–situ* laser remelting on structural evolution and high–temperature tribological properties of plasma sprayed Cu11.85Al3.2Mn0.1Ti coating, *Materials Today Communications*, vol. **39**, p. 109085, 2024.

Cherenda, N.N., Basalai, A.V., Uglov, V.V., Laskovnev, A.P., Astashynski, V.M., Kuzmitski, A.M., Phase composition and mechanical properties of Cu-Ti alloys synthesized in the surface layer of copper by plasma impact on the Ti/Cu system, *Vacuum*, Vol. **167**, pp. 452-458, (2019).

Cherenda, N. N., Laskovnev, A. P., Basalai, A. V., Uglov, V. V., Astashynski, V. M., Kuzmitski, A. M., Erosion of Materials under the Effect of Compression Plasma Flows, *Inorganic Materials: Applied Research*, Vol. **6**, No. 2, pp. 114–120, 2015.

Cherenda, N., Leivi, A., Petukh, A., Uglov, V., Grigoriev, S., Vereschaka, A., Astashynski, A., Kuzmitski, A.,. Modification of Ti-6Al-4V titanium alloy surface relief by compression plasma flows impact, *High Temperature Material Processes*, vol. **28**, no. 2, pp. 7–24, 2024.

Cherenda, N.N., Petukh, A.B., Kuleshov, A.K., Rusalsky, D.P., Bibik, N.V., Uglov, V.V., Grigoriev, S.N., Vereschaka, A.A., Astashynski, V.M., Kuzmitski, A.M., Scratch testing of ZrN coating on Ti-6Al-4V titanium alloy surface preliminary treated by compression plasma flows impact, *High Temperature Material Processes*, vol. **28**, no. 3, pp. 25–36, 2024.

Cherenda, N.N., Shimanskii, V. I., Uglov, V. V., Astashinskii, V. M., Ukhov, V. A., Nitriding of Steel and Titanium Surface Layers under the Action of Compression Plasma Flows. *Journal of*

Surface Investigation. X-ray, Synchrotron and Neutron Techniques, vol. **6**, no. 2, pp. 319-325, 2012.

Fattah-alhosseini, A., Molaei, M., A review of functionalizing plasma electrolytic oxidation (PEO) coatings on titanium substrates with laser surface treatments, *Applied Surface Science Advances*, vol. **18**, p.100506, 2023.

Grigoriev, S., Vereschaka, A., Uglov, V., Milovich, F., Tabakov, V., Cherenda, N., Andreev, N., Migranov, M., Influence of the tribological properties of the Zr,Hf-(Zr,Hf)N-(Zr,Me,Hf,Al)N coatings (where Me is Mo, Ti, or Cr) with a nanostructured wear-resistant layer on their wear pattern during turning of steel. *Wear*, vol. **518-519**, p. 204624, 2023.

Grigoriev, S., Volosova, M., Bublikov, Y., Sotova, C., Milovich, F., Shmakov, I., Vereschaka, A., Study of the Features of Coating Deposition on a Carbide SubstrateUsing Preliminary Etching with Glow Discharge Plasma, *Preprints.org*, doi: 10.20944/preprints202407.2206.v1, 2024.

Guan, Q., Han, J., Zhou, S., Guan, J., Zhang, C., Cao, F., Chen, X., Improved mechanical and tribological properties of TiAlN coatings by highcurrent pulsed electron beam irradiation, *International Journal of Refractory Metals and Hard Materials*, vol. **118**, p. 106435, 2024.

Koshuro, V., Osipova, E., Markelova, O., Fomina, M., Zakharevich, A., Pichkhidze, S., Fomin, A., Titanium oxide coatings formed by plasma spraying followed by induction heat treatment, *Ceramics International*, vol. **49**, no. 2, pp. 2034-2043, 2023.

Leyvi, A.Ya., Cherenda, N.N., Uglov, V.V., Yalovets, A.P., The impact of a shock-compressed layer on the mass transfer of target material during processing compression plasma flows, *Resource-Efficient Technologies*, vol. **3**, pp. 222–225, 2017.

Leyvi A.Y., Yalovets, A.P., Coating of a substrate with surface preliminarily treated with intensive flows of high-speed electrons and plasma using a magnetron, *J. Phys.: Conf. Ser.*, vol. **830**, p. 012111, 2017.

Manory, R.R., Liu, L.J., Sood, D.K., Shao, Z.M., Kylner, C., Braun, M., Post-deposition treatments of hard coatings. Part II: Ion beam treatments of TiN and related coatings, *Surface and Coatings Technology*, vol. **70**, pp. 1-7, 1994.

Martynenko, Yu.V., Metal erosion under plasma flow typical for ITER transient regimes *Physics Procedia*, Vol. **71**, pp. 9 – 13, 2015.

Mirhosseini, S., Mahboubi, F., Azadfalah, M., Effect of different plasma nitriding durations on the tribological characteristics of nickel-boron-nanodiamond electroless nanocomposite coatings, *Surface and Coatings Technology*, vol. **476**, p. 130181, 2024.

Niksefat, V., Mahboubi, F., Tribological performance of plasma-nitrided self-lubricant electroless Ni-B-graphite composite coatings, *Tribology International*, vol. **198**, p. 109905, 2024.

Petrov, P., Dechev, D., Ivanov, N., Hikov, T., Valkov, S., Nikolova, M., Yankov, E., Parshorov, S., Bezdushnyi, R., Andreeva, A., Study of the influence of electron beam treatment of Ti5Al4V substrate on the mechanical properties and surface topography of multilayer TiN/TiO2 coatings, *Vacuum*, vol. **154**, pp. 264-271, 2018.

Proskurovsky, D.I., Rotshtein, V.P., Ozur, G.E., Ivanov, Yu.F., Markov, A.B., Physical foundations for surface treatment of materials with low energy, high current electron beams, *Surface and Coatings Technology*, vol. **125**, pp. 49–56, 2000.

Remnev, G.E., Isakov, I.F., Opekounov, M.S., Matvienko, V.M., Ryzhkov, V.A., Struts V.K., Grushin, I.I., Zakoutayev, A.N., Potyomkin, A.V., Tarbokov, V.A., Pushkaryov, A.N., Kutuzov, V.L., Ovsyannikov, M.Yu., High intensity pulsed ion beam sources and their industrial applications, *Surface and Coatings Technology*, vol. **114**, pp. 206–212, 1999.

Sharma, P., Ponte, F., Lima, M.J., Figueiredo, N.M., Ferreira, J., Carvalho, S., Plasma etching of polycarbonate surfaces for improved adhesion of Cr coatings, *Applied Surface Science*, vol. **637**, p. 157903, 2023.

Schulz, A., Stock H.-R., Mayr, P., Physical vapour deposition of TiN hard coatings with additional electron beam heat treatment, *Materials Science and Engineering A*, vol. **140**, pp. 639-646, 1991.

Szajna, E., Moskal, G., Tupaj, M., Dresner, J., Dudek, A., Szymański, K., Tomaszewska, A., Trzcionka-Szajna, A., Mikuśkiewicz, M., Łysiak, K., The influence of laser remelting on microstructural changes and hardness level of flame-sprayed NiCrBSi coatings with tungsten carbide addition, *Surface and Coatings Technology*, vol. **478**, p. 130403, 2024.

Tereshin, V.I., Garkusha, I.E., Bandura, A.N., Byrka, O.V., Chebotarev, V.V., Makhlaj, V.A., Solyakov, D.G., and Wuerz, H., Influence of plasma pressure gradient on melt layer macroscopic erosion of metal targets in disruption simulation experiments, *J. Nucl. Mater.*, vol. **313–316**, pp. 685–689, 2003.

Weigel, K., Bewilogua, K., Keunecke, M., Bräuer, G., Grumbt, G., Zenker, R., Biermann, H., Effects of electron beam treatment on Ti(1x)AlxN coatings on steel, *Vacuum*, vol. **107**, pp. 141-144, 2014.

Vereschaka, A., Tabakov, V., Grigoriev, S., Sitnikov, N., Milovich, F., Andreev, N., Sotova, C., Kutina, N., Investigation of the influence of the thickness of nanolayers in wear-resistant layers of Ti-TiN-(Ti,Cr,Al)N coating on destruction in the cutting and wear of carbide cutting tools. *Surf. Coat. Technol.*, vol. **385**, p. 125402, 2020.

Zenker, R., Sacher, G., Buchwalder, A., Liebich, J., Reiter, A., Häßler, R., Hybrid technology hard coating – Electron beam surface hardening, *Surface & Coatings Technology*, vol. **202**, pp. 804–808, 2007.

Zhang, K., Guo, X., Wang, C., Liu, F., Sun, L., Effect of plasma-assisted laser pretreatment of hard coatings surface on the physical and chemical bonding between PVD soft and hard coatings and its resulting properties, *Applied Surface Science*, vol. **509**, p. 145342, 2020.